applied sciences

MDPI

Article

Application of Component-Based Mechanical Models and Artificial Intelligence to Bolted Beam-to-Column Connections

Iman Faridmehr [1], Mehdi Nikoo [2], Raffaele Pucinotti [3] and Chiara Bedon [4,*]

[1] Institute of Architecture and Construction, South Ural State University, 454080 Chelyabinsk, Russia; faridmekhri@susu.ru
[2] Young Researchers and Elite Club, Ahvaz Branch, Islamic Azad University, Ahvaz 61349-37333, Iran; m.nikoo@iauahvaz.ac.ir
[3] Department of Mechanics and Materials, University of Reggio Calabria, 89124 Reggio Calabria, Italy; raffaele.pucinotti@unirc.it
[4] Department of Engineering and Architecture, University of Trieste, Via Valerio 6/1, 34127 Trieste, Italy
* Correspondence: chiara.bedon@dia.units.it; Tel.: +39-040-558-3837

Abstract: Top and seat beam-to-column connections are commonly designed to transfer gravitational loads of simply supported steel beams. Nevertheless, the flexural resistance characteristics of these type of connections should be properly taken into account for design, when a reliable analysis of semi-rigid steel structures is desired. In this research paper, different component-based mechanical models from Eurocode 3 (EC3) and a literature proposal (by Kong and Kim, 2017) are considered to evaluate the initial stiffness ($S_{j,ini}$) and ultimate moment capacity (M_n) of top-seat angle connections with double web angles (TSACWs). An optimized artificial neural network (ANN) model based on the artificial bee colony (ABC) algorithm is proposed in this paper to acquire an informational model from the available literature database of experimental test measurements on TSACWs. In order to evaluate the expected effect of each input parameter (such as the thickness of top flange cleat, the bolt size, etc.) on the mechanical performance and overall moment–rotation (M–θ) response of the selected connections, a sensitivity analysis is presented. The collected comparative results prove the potential of the optimized ANN approach for TSACWs, as well as its accuracy and reliability for the prediction of the characteristic (M–θ) features of similar joints. For most of the examined configurations, higher accuracy is found from the ANN estimates, compared to Eurocode 3- or Kong et al.-based formulations.

Keywords: top-seat angle connections (TSACW); component-based models; initial stiffness; ultimate moment capacity; moment-rotation relation; artificial neural network (ANN); sensitivity analysis (SA)

Citation: Faridmehr, I.; Nikoo, M.; Pucinotti, R.; Bedon, C. Application of Component-Based Mechanical Models and Artificial Intelligence to Bolted Beam-to-Column Connections. *Appl. Sci.* **2021**, *11*, 2297. https://doi.org/10.3390/app11052297

Academic Editors: César M. A. Vasques and Alkiviadis Paipetis

Received: 1 February 2021
Accepted: 2 March 2021
Published: 5 March 2021

Publisher's Note: MDPI stays neutral with regard to jurisdictional claims in published maps and institutional affiliations.

1. Introduction

Bolted top-seat angle connections without (TSAC) or with web angles (TSACW) have been extensively used in steel and composite structures, because of their relatively high moment capacity and easy construction. These types of connections are mainly designed to resist gravity loads of determinate steel beams. A schematic layout is proposed in Figure 1. Based on the AISC standard [1], a given TSACW is classified as a semi-grid beam-to-column connection, in which the moment–rotation (M–θ) behavior needs to be considered in the overall force distribution and structural analysis. Accordingly, there are no doubts on the necessity to accurately predict the (M–θ) behavior of TSACW joints.

The (M–θ) behavioral trends of steel connections represent essential features of their response, and in particular with regard to the initial stiffness $S_{j,ini}$, maximum moment capacity M_n, and maximum rotation θ_u. Once these features are correctly estimated, a reliable simulation of the actual behavior toward the optimum design of structures would be possible. The behavior of TSACs and TSACWs has been investigated and equivalent equations have been proposed to simulate their mechanical behavior for applications

to steel frames [2–6]. In parallel to TSACWs, a similar solution has a key role also for "modular buildings", namely, off-site prefabricated building modules in which the primary structure consists of steel frames, whose construction has become increasingly popular due to the advantages, including reduced resource wastage and improved quality [7–10]. The typical connection takes the form of a bolted connection with a plug-in device or a bolted connection with a rocket-shaped tenon. Being classified as "bolted", these connections have the advantages of reduced site work and demountability.

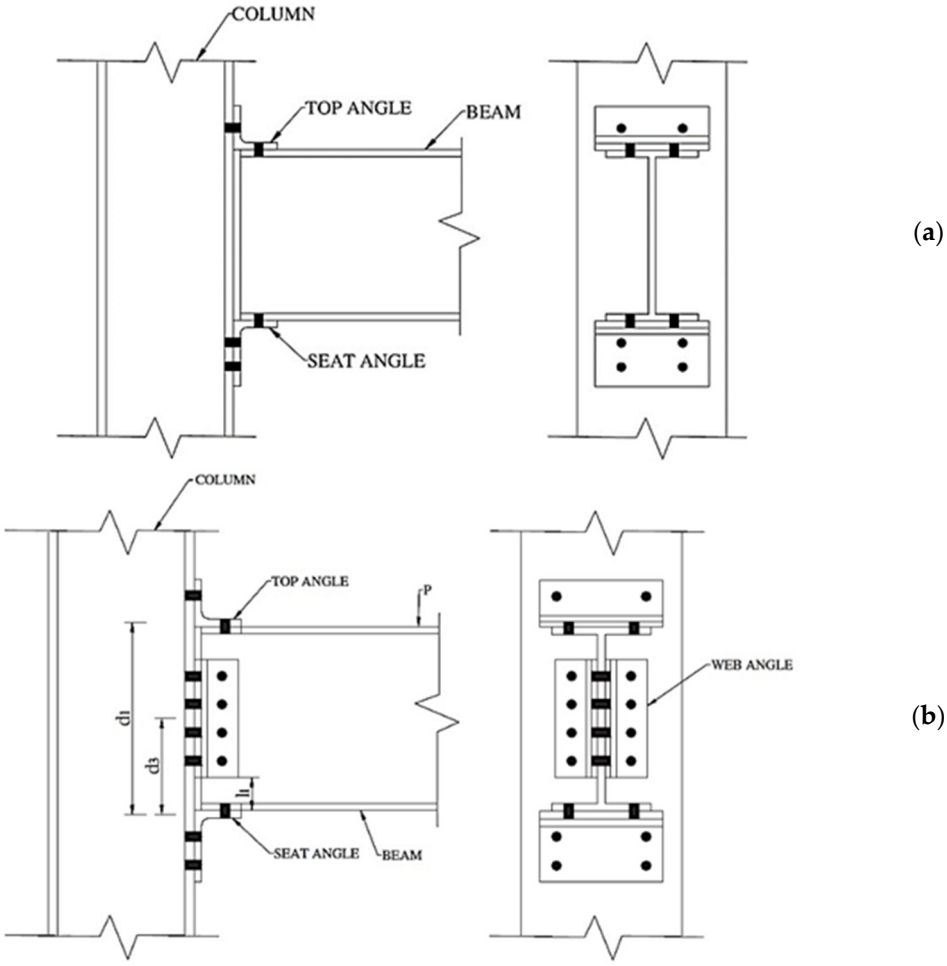

Figure 1. Reference configurations for (**a**) top-seat angle connections without (TSAC) or (**b**) with web angles (TSACW).

In both the cases, the mechanical properties of connections have a great influence on the strength and stability of the structural system to which they belong. An unrealistic design of connections may negatively affect the serviceability of the structure as a whole, due to the occurrence of large deflections. Deformations in connection components as a result of local buckling phenomena is also a common reason for the failure of these connections. The key role of connections for modular buildings has been recognized to affect the overall structural performance of modular systems. Despite this importance, the design of reliable connections is still identified as a major challenge, and prevalent knowledge of their structural performance is still limited [11,12].

In this paper, an original study is presented for TSACWs. An artificial neural network (ANN) model able to capture the underlying mechanism and to accurately estimate both the initial stiffness $S_{j,ini}$ and the ultimate moment capacity M_n for TSACWs is proposed. To this aim, two reference calculation approaches are taken into account from the literature, and investigated in detail, namely, (i) the mechanical component-based model approach

proposed by Eurocode 3 ("EC3" [13]) and (ii) the analytical formulation proposed by Kong and Kim in [14] ("KK"). Since the $S_{j,ini}$ and M_n features for a given TSACW are the most influential parameters that affect the overall mechanical characterization of a given bolted beam-to-column connection, these two selected properties are preliminarily calculated based on the selected "EC3" and "KK" formulations, and compared against each other, with the support of experimental data from the literature (77 specimens in total). Successively, a comprehensive ANN approach, combined with a metaheuristic artificial bee colony (ABC) algorithm, is developed in this paper to extract an informational model for TSACWs. A major advantage for the definition of the proposed model is given by the support of experimental data from the literature, and sensitivity analysis to assess the collected comparative results. The potential and limits of each scheme, as well as the original ABC-ANN for TSACW joints, are hence discussed in detail.

2. State of the Art

Different parameters contribute to the (M–θ) behavioral characterization of bolted connections, as shown in Figure 2 [15–20], and it is thus first necessary to use reliable modeling techniques. In the case of modular steel buildings, non-linear link elements are generally incorporated for computational efficiency, where the bending moment, shear, axial force, and corresponding moment–rotation (M–θ) curves are simplified and included as spring elements. Nevertheless, since the knowledge of the structural behavior of modular steel buildings is limited, the simplified models for the force–displacement and moment–rotation curves are not well established. Therefore, the intrinsic uncertainty can lead to excessively conservative design practices, requiring additional investigations on the topic.

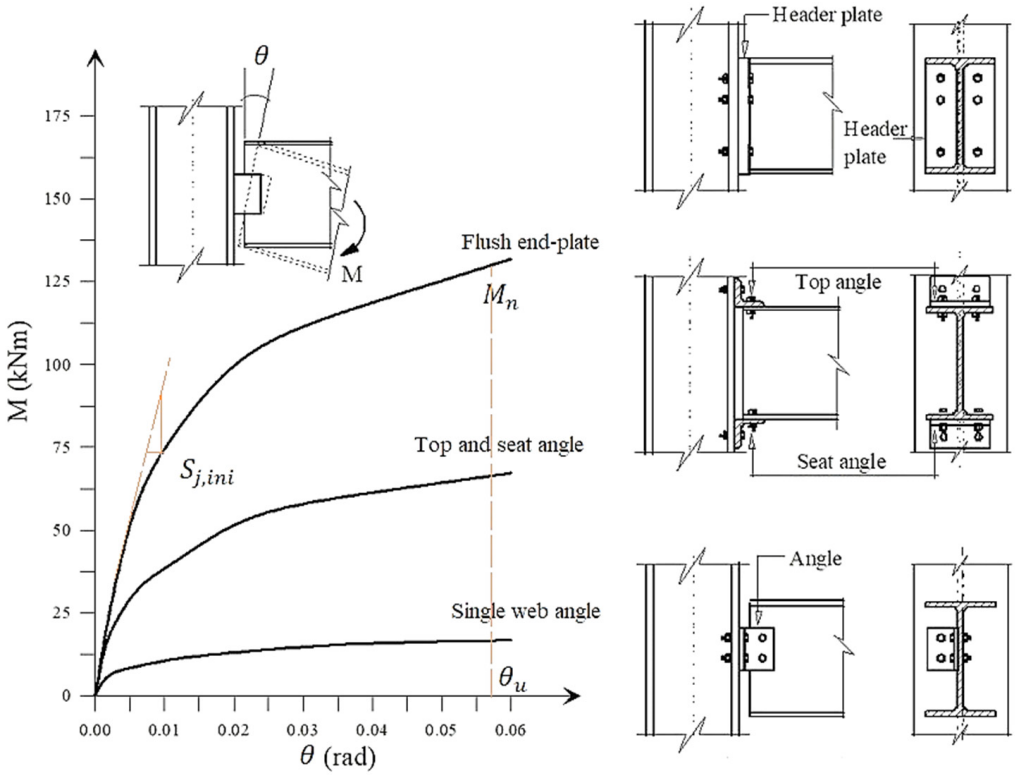

Figure 2. Moment–rotation curve of common types of beam-to-column connections (adapted from [5] under the terms and conditions of a Creative Commons Attribution License (CC BY)).

Extended literature studies are indeed available for TSACs and TSACWs. To simulate the beam-to-column connection behavior, apart from experimental tests, three different modeling options are introduced in the form of analytical or empirical models [21], advanced finite element (FE) models [22–24], and component mechanical models [25,26].

Analytical and empirical models naturally extract simple mathematical expressions, and thus typically facilitate their application in practice, with a reasonable level of accuracy. On the other hand, by applying advanced FE methods, it is possible to simulate more precisely the complex non-linear beam-to-column connection response. Some limitations are unavoidably introduced in terms of high computational cost and sophisticated preparation process (assembly, calibration, etc.). Component-based mechanical models, finally, consider an assembly of rigid elements and equivalent springs relay on the two previous modeling approaches, considering computational complexity and reliability.

Several research studies have documented the (M–θ) performance of TSACWs, especially through extended experimental investigations. In 1985 and 2000, respectively, Azizinamini and Radziminski [25] and Calado et al. [15] experimentally investigated the (M–θ) behavior of TSACW specimens under monotonic and cyclic loading. The hysteresis behavior of TSACW specimens was investigated in several cited projects. The presented results indicated that the main sources of plastic deformation are typically located in the top and bottom cleats, which represent the governing components. In addition, the same studies proved a limited influence of the column size on the overall hysteretic performance of the examined connections. A considerable number of literature studies has also been published in support of the prediction of the (M–θ) behavior, initial stiffness, and ultimate strength of TSACW systems through various mechanical and analytical models. In 1987, Azizinamini et al. [27] proposed a set of relevant equations to predict initial stiffness. Kishi et al. [28,29] presented an analytical model to estimate both the initial stiffness and ultimate moment capacity of TSACWs through cantilever beam theory. In more detail, a three-parameter power model was discussed in [29], in which the elastic stiffness and ultimate moment capacity of connection of TSACWs were estimated by a simple analytical method. Pucinotti [30] proposed a simplified mechanical model along with relevant initial stiffness and ultimate moment equations. A three-linear (M–θ) constitutive law based on the fiber element formulation was proposed by Shen and Astaneh-Asl [31]. In that study, two possible mechanisms were considered, according to the strength of the angles relative to the bolt. They concluded that plastic hinges were crated at the leg of the angles in thinner top cleats, while the plastic hinge was generally found to appear at the central line of the column bolts, along with plastic deformations of the bolts. A mechanical model for estimating the inelastic cyclic (M–θ) relationship of TSACWs was proposed by De Stefano et al. [32]. Currently, by the advances in computer technologies, there is a large volume of published studies on (M–θ) behavior of beam-to-column connections through the FE method. For example, Danesh et al. [33] investigated the effect of shear force on the expected initial stiffness. Pirmoz et al. [34] focused on the effect of web angle on the (M–θ) behavior. Salem et al. [35] conducted parametric research on the prying action of bolts. Their study indicated that the prying force of top cleat and column flange bolts is found to increase by decreasing the vertical leg of the top cleat. Collectively, all the mentioned studies (and others) outline a set of different methodologies in support of a reliable (M–θ) modeling and mechanical characterization of beam-to-column connections.

Among the multitude of research studies that have been done on TSACs or TSACWs, traditional experimental or numerical methods are used in most of the cases. The current investigation, in this regard, applies ANN techniques for the analysis of this type of connection. ANNs are largely used for solving complex civil engineering (and other) problems, and their application has increased significantly in the last few years. ANNs can be effectively applied for predictive modeling in different engineering fields, especially in those cases where some prior (experimental or numerical) analyses are already available. The origins of ANNs can be found in the field of biology, where the biological brain consists of billions of highly interconnected neurons, forming a neural network.

A validated informational method is developed in this paper, to provide an alternative tool that could be used to model the complex structural and material behavior in TSACWs that cannot be easily approximated and generalized by conventional approaches. The information about the underlying mechanics for TSACWs is extracted from the observed ex-

perimental data of the literature, which are processed in neural networks and subsequently trained with optimization techniques.

3. Data Bank Development

Having recognized that different parameters contribute to the (M–θ) behavioral characterization of bolted beam-to-column connections, it is first fundamental to develop a consistent data bank of test results for the examined connection typology. Experimental investigations and their results—when correctly extracted—notoriously allow a more robust and accurate classification of different behavioral features for beam-to-column connections, including $S_{j,ini}$ and M_n, but also hardening, non-linearities, progressive damage and degradation of mechanical parameters, rotation capacity, failure mechanism, and sequence. The same database is also strictly necessary for the development of the ANN model herein proposed.

In this paper, the preliminary verification of the component-based mechanical model for bolted TSACWs, as well as the training data to develop the ANN model, is carried out with the support of experimental data from the literature. Table 1 presents a short summary of the major geometrical and material properties for the examined TSACWs. The full data of TSACW specimens are available in [27,36,37].

Table 1. Geometrical and mechanical characteristics of selected TSACW specimens.

Test	Beam	Column	Size of Bolts (mm)	Top Cleat (mm)	Web Cleat (mm)	Yield Stress of Angle (N/mm^2)
8S1	H210 × 134 × 6.4 ×10.2	H310 × 254 × 9.1 × 16.3	19.1	L152 × 89 × 7.9	L102 ×89 × 6.4	285.4
8S2	H210 × 134 × 6.4 ×10.2	H310 × 254 × 9.1 × 16.3	19.1	L152 × 89 × 9.5	L102 × 89 × 6.4	285.4
8S3	H210 × 134 × 6.4 × 10.2	H310 × 254 × 9.1 × 16.3	19.1	L152 × 89 × 7.9	L102 × 89 × 6.4	285.4
8S4	H210 × 134 × 6.4 × 10.2	H310 × 254 × 9.1 × 16.3	19.1	L152 × 152 × 9.5	L102 × 89 × 6.4	285.4
8S5	H210 × 134 × 6.4 × 10.2	H310 × 254 × 9.1 × 16.3	19.1	L152 × 102 × 9.5	L102 × 89 × 6.4	285.4
8S6	H210 × 134 × 6.4 × 10.2	H310 × 254 × 9.1 × 16.3	19.1	L152 × 102 × 7.9	L102 × 89 × 6.4	285.4
8S7	H210 × 134 × 6.4 × 10.2	H310 × 254 × 9.1 × 16.3	19.1	L152 × 102 × 9.5	L102 × 89 × 6.4	285.4
8S8	H210 × 134 × 6.4 × 10.2	H310 × 254 × 9.1 × 16.3	22.2	L152 × 89 × 7.9	L102 × 89 × 6.4	277
8S9	H210 × 134 × 6.4 × 10.2	H310 × 254 × 9.1 × 16.3	22.2	L152 × 89 × 9.5	L102 × 89 × 6.4	277
8S10	H210 × 134 × 6.4 × 10.2	H310 × 254 × 9.1 × 16.3	22.2	L152 × 89 × 12.7	L102 × 89 × 6.4	277
14S1	H358 × 172 × 7.9 × 13.1	H323 × 310 × 14 × 22.9	19.1	L152 × 102 × 9.5	L102 × 89 × 6.4	285
14S2	H358 × 172 × 7.9 × 13.1	H323 × 310 × 14 × 22.9	19.1	L152 × 102 × 12.7	L102 × 89 × 6.4	365
14S3	H358 × 172 × 7.9 × 13.1	H323 × 310 × 14 × 22.9	19.1	L152 × 102 × 9.5	L102 × 89 × 6.4	285
14S4	H358 × 172 × 7.9 × 13.1	H323 × 310 × 14 × 22.9	19.1	L152 × 102 × 9.5	L102 × 89 × 9.5	285
14S5	H358 × 172 × 7.9 × 13.1	H323 × 310 × 14 × 22.9	19.1	L152 × 102 × 9.5	L102 × 89 × 6.4	277
14S6	H358 × 172 × 7.9 × 13.1	H323 × 310 × 14 × 22.9	19.1	L152 × 102 × 12.7	L102 × 89 × 6.4	277
14S8	H358 × 172 × 7.9 × 13.1	H323 × 310 × 14 × 22.9	19.1	L152 × 102 × 15.9	L102 × 89 × 6.4	277
14S9	H358 × 172 × 7.9 × 13.1	H323 × 310 × 14 × 22.9	19.1	L152 × 102 × 12.7	L102 × 89 × 6.4	277

4. Component-Based Mechanical Models for TSACWs

4.1. Initial Stiffness

The initial stiffness $S_{j,ini}$ of bolted connections is one of the most important parameters for the characterization of their (M–θ) response. There is a large volume of published studies investigating $S_{j,ini}$ of bolted beam-to-column connections. The first deep discussion and analysis about $S_{j,ini}$ emerged in the 1980s with the research studies by Azizinamini et al. [27]. The authors proposed a beam model dividing the leg of the top cleat flange into two types of beam segments, flexible and rigid sections. Relevant equations of practical use have been presented to estimate $S_{j,ini}$ for TSACWs. Later, Kishi and Chen [29] presented a new equation that was developed according to the cantilever beam model.

The EC3 standard document [13]—Annex J—implemented a component method to estimate the $S_{j,ini}$ of TSACs. In this method, the connection behavior is simulated by a series

of different components, each one represented in the form of an elastic spring with specific stiffness and strength. The overall initial stiffness of the connection is hence notoriously estimated by assembling all the springs in a parallel series configuration, as shown in Figure 3.

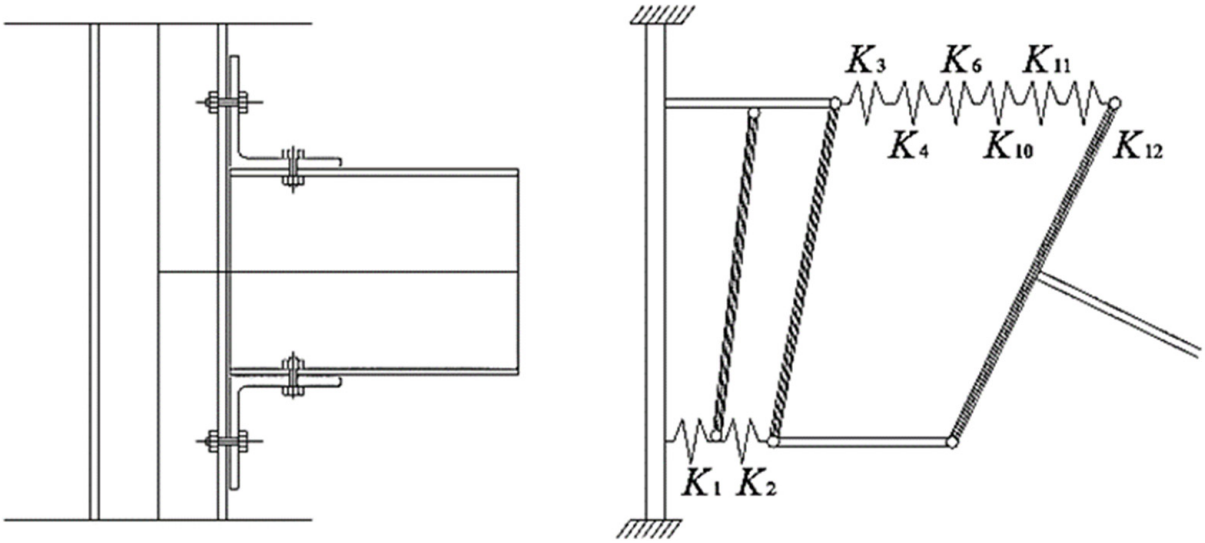

Figure 3. Component-based modeling of TSAC.

In the EC3, the input stiffness coefficients that must be considered are associated with the column shear panel zone (K_1), the column flange in tension (K_3), the column flange in compression (K_2), the flexural stiffness of column flange (K_4), the top cleat flexural stiffness (K_6), the tensile stiffness of bolts (K_{10}), and, for non-preloaded bolts, their shear stiffness (K_{11}) and their bearing stiffness (K_{12}). In conclusion, $S_{j,ini}$ of TSACs is given by:

$$S_{j,\,ini} = \frac{E\,z^2}{\sum_{i=1}^{n} 1/K_i} \tag{1}$$

where E is Young's modulus, z is the lever arm, K_i is the i-th component stiffness coefficient, and n is the number of joint components, as in Figure 3. Finally, z should be taken as the distance from the bolt-row in tension and mid-thickness of the leg of the seat cleat on the compression flange.

While the above formulation is widely used in practice, the EC3 formulation does not include a mechanical model for TSACWs. Accordingly, an extension of EC3 for TSACWs is proposed in this paper. For a bolt-row in a web cleat, the stiffness illustrated in Figure 4 should be considered.

The overall stiffness of basic components illustrated in Figure 4 is represented by a single equivalent stiffness coefficient k_{eq}, that can be calculated as:

$$k_{eq} = \frac{\frac{S_{j,\,ini}}{Ez} + \sum k_{eff,\,r} z_r}{z_{eq}} \tag{2}$$

where $S_{j,ini}$ is again the initial stiffness for TSACs, while z_r represents the distance between the center of the compression cleat and the bolt-row r of the web cleat.

Moreover:

$$k_{eff,\,r} = \frac{1}{\sum_i 1/k_{i,\,r}} \tag{3}$$

where $k_{i,r}$ is the stiffness coefficient representing component i relative to bolt-row r, and:

$$z_{eq} = \frac{\frac{S_{j,\,ini}}{E} + \sum_r k_{eff,\,r} z_r^2}{\frac{S_{j,\,ini}}{Ez} + \sum_r k_{eff,\,r} z_r} \tag{4}$$

In conclusion, the initial stiffness of TSACWs can be calculated as:

$$S_{j,\,ini} = \frac{E z_{eq}}{k_{eq}} \tag{5}$$

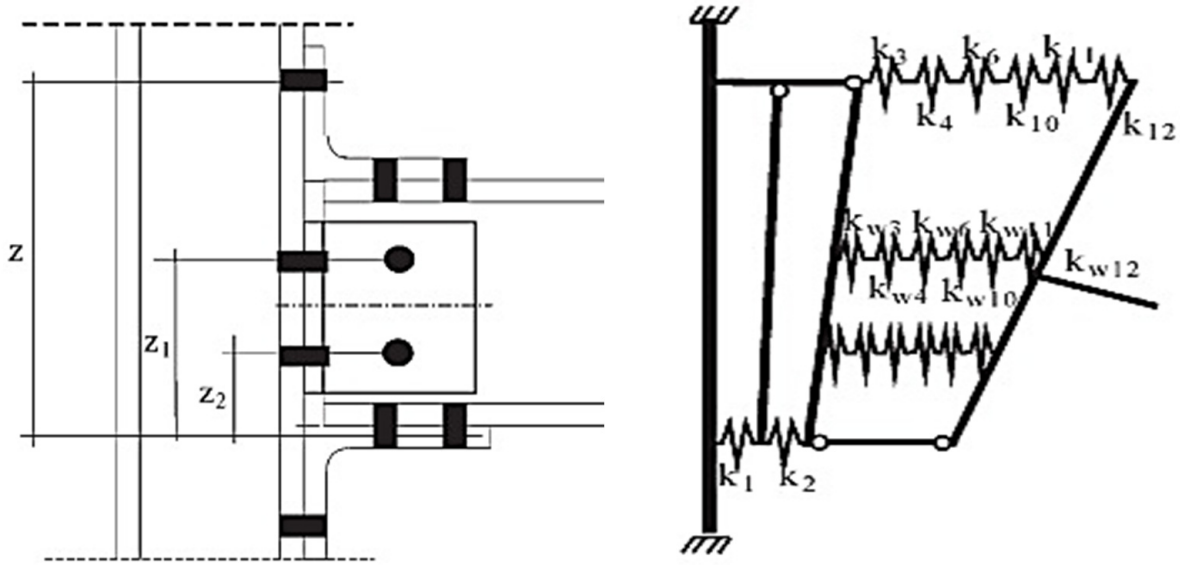

Figure 4. Proposed extension of component-based model for TSACW.

Kong and Kim [14] have used curve fitting software to obtain the effects of top and seat angles on the $S_{j,ini}$ value of TSACWs. Past literature studies also recognized that $S_{j,ini}$ correlates well with correlates the angle thickness, the length of the top angle, the height of the beam, the thickness of the column flange, the fillet size of the top angle, the thickness of the beam web, the gauge distance, and the diameter of bolts. In [14], therefore, a semi-empirical equation has been proposed as:

$$S_{j,\,ini} = \frac{0.49 E l_t t^3{}_t \left(d + \frac{t_t}{2} + \frac{t_s}{2} + 2k_t\right)}{\left(g_t - t_t - \frac{d_b}{2}\right)^2} \frac{t_{cf}}{t_t} \frac{t_{bw}}{t_t} \left(\frac{d}{t_t}\right)^{0.3} + \frac{0.312 n \alpha E l_p{}^2 t_a}{(1+v) g_c} \tag{6}$$

In Equation (6), E is the previously defined Young's modulus; l_t is the length of top angle; t_t is the top angle thickness; t_s is the thickness of seat angle; d is the height of beam; k_t is the fillet size of top angle; t_{cf} is the thickness of column flange; t_{bw} is the thickness of beam web; g_t is the distance from top angle heel to the center of bolts; d_b is the diameter of bolts; n is the number of bolts; α = 1.0 mm; l_p is the angle length of the web; ta is the angle thickness of web; v is Poisson's ratio; and $g_c = g_1 - t_a$, as shown in Figure 5.

4.2. Ultimate Moment Capacity

The ultimate moment capacity M_n is one of the well-known fundamental parameters that affects the overall response of bolted beam-to-column connections. Several literature studies on TSACW specimens suggest that a rotation of 0.03 rad is sufficient to experience the full plastic moment capacity M_p of the connected beam [38]. The American Institute of Steel Construction [39], in this regard, recommends considering a relatively low rotation

during the analysis and design process for this connection typology. Accordingly, the amplitude of 0.03 rad is defined as the maximum rotation capacity of TSACWs.

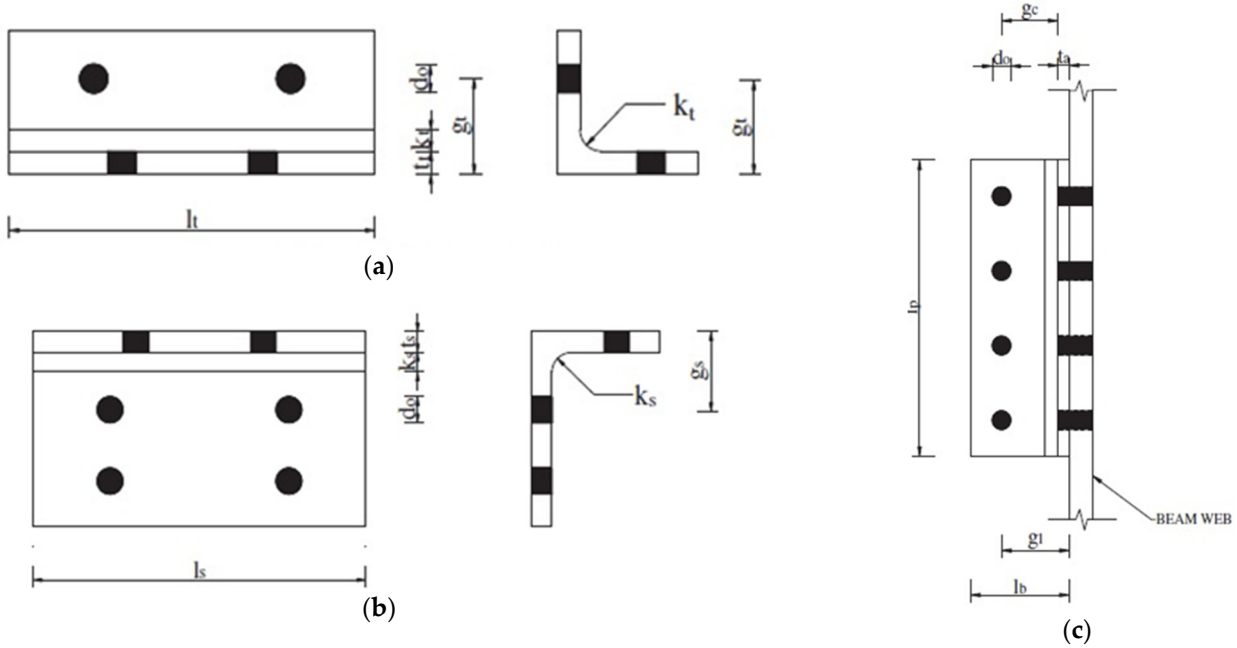

Figure 5. Geometrical parameters of the reference TSACW: (**a**) top angle, (**b**) seat angle, (**c**) web angle. Reproduced from [14] with permission from Elsevier, copyright agreement with license number 5011231057466, February 2021.

The component-based method can be extended to estimate the ultimate moment capacity M_n of TSACWs, as far as the contribution of influencing components is properly considered. These all affect the overall TSACW flexural resistance and are represented by: the column web panel in shear, the column web in compression, the column web in tension, the column flange in bending, the top cleat in bending, the web cleat in bending, the bolts in tension or in shear, the beam web in tension, and the beam flange and web in compression. Past research studies proposed different mechanical models to calculate M_n [30,40,41]. In most of those proposals, the failure of the top, seat, and web cleat's leg under maximum moment was only recognized, while other failure mechanisms (such as the failure of one or more bolts) were fully disregarded. In 2005, the EC3 standard [13] defined the required ultimate moment capacity M_n of TSACs and TSACWs as:

$$M_n = F_{Rd} Z \tag{7}$$

where Z is the lever arm and F_{Rd} is the design resistance of weak joint components. The second term can be governed by one of the following mechanisms: top cleat in bending ($F_{tc,Rd}$), bolts in tension, beam flange in tension and compression, and beam web in tension.

For a TSAC with a single-web cleat, Kishi and Chen [29], in 1990, elaborated a model proposal for the detection of collapse mechanisms. Kong and Kim [14] further extended the method from [29], and presented a formulation for TSACWs:

$$M_n^{top-seat} = M_{os} + M_p + V_{pt} d_2 + V_{pa} d_4 \tag{8}$$

In Equation (8), M_{os} is the plastic moment capacity of the seat angle; M_p is the plastic moment capacity of the top angle; V_{pt} is the ultimate shear force acting on the top angle; d_2 is a parameter related to the depth of the beam and thickness of top and seat cleats; V_{pa} is a parameter that depends on the ultimate shear force at the upper and lower edges of the web cleat; and d_4, finally, is the distance between plastic shear at the lower edge of the web cleat to the center of compression. These parameters are schematized in Figure 6.

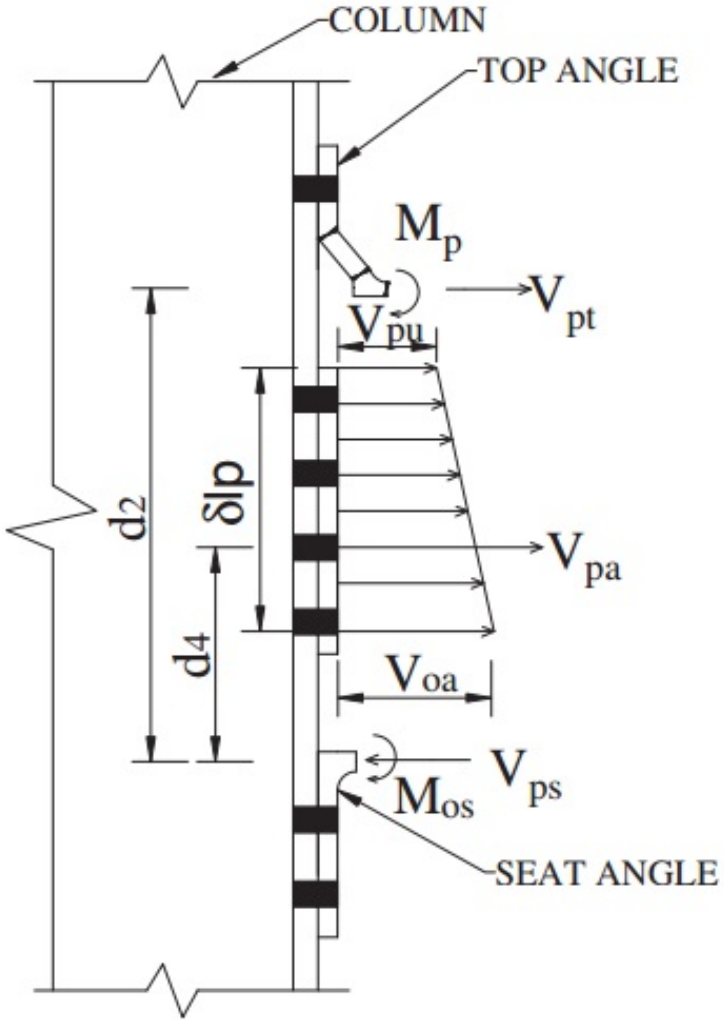

Figure 6. Collapse mechanism for TSACW. Reproduced from [14] with permission from Elsevier, copyright agreement with license number 5011231057466, February 2021.

5. Informational Based Modeling

An informational-based method recognizes, as an alternative method to simulate the complex structural and material behavior, that conventional methods are not simply estimated. This alternative method simulates the behavior by the information provided by selected tested specimens. Accordingly, this is an essential evolution from mathematical equations to preserve data that contain the necessary information on mechanical characteristics. In this approach, the underlying mechanics information is extracted from the experimental test data and processed in the ANN program.

Among numerous structures of ANNs that have been studied, the most widely used one is represented by the multi-layered feed-forward (FF) network, which is the structure implemented in the current investigation. Among others, FF is the oldest and simplest of existing ANNs, representing the most popular class of ANNs for its computational efficiency [42]. The main structure of a neural network is usually made up of three distinct layers, and never cycles. According to the literature, three-layer FF networks are found to be sufficient in civil engineering practices [43]. The input layer is where the data are introduced to the model, the hidden layer is where the data are processed, and the output layer is where the model results are generated. Each layer is made up of nodes called neurons [44]. Apart from the neurons in the input layer, which only receive and transmit incoming signals to other neurons in the hidden layer, each neuron in the other layers consists of three main components, weights, bias, and an activation function, which can

be linear or non-linear. After determining the network topology, including the number of layers, the number of neurons, the type of transmission function, and the network learning algorithm, modeling for data can be started [45]. During the analysis of the model using learning algorithms, the number of errors can be reduced by adjusting weights and bias in each neuron. For this purpose, the Levenberg–Marquardt algorithm has been used in modeling the neural network due to its high speed and accuracy. The training algorithm distributes the network error to achieve optimal or minimum error [46,47].

5.1. Artificial Bee Colony (ABC) Algorithm

The artificial bee colony (ABC) algorithm is an optimization algorithm based on the bee population's collective intelligence and intelligent behavior in finding food [44]. In its primary model, the algorithm performs a neighborhood search combined with a random search, and can be used for either combined or functional optimization [48].

In the ABC algorithm, the colony consists of three groups of bees: employed, onlookers, and scout bees. The first and the second half of the colony consist of employed artificial bees and onlookers, respectively. There is only one employed bee for every food source. In this algorithm, moreover, a scout is representative of an employed bee of an abandoned food source. Overall, the search process in ABC can be summarized as follows [49,50]:

- A food source is determined by employed bees in their memory within the neighborhood.
- The collected information of food sources by employed bees is shared with onlookers within the hive, and subsequently, the optimum food sources will be selected by onlookers.
- A food source will be selected by onlookers themselves within the neighborhood of the food sources.
- An employed bee becomes a scout once the food source has been abandoned and starts to search for a new food source randomly.

5.2. Training the ANN and Methodology

To train the artificial neural network, a total number of 77 specimens from [36] and [37] was considered in this study, in order to determine two outputs of $S_{j,ini}$ and ($M_n/M_{p,beam}$). Up to ≈ 80% of the selected samples (62) was used for training, while 20% (15 specimens) was used for testing the network.

Accordingly, several variables were introduced as input parameters for the model, including:

- the moment inertia ratio of the column to the connected beam (I_{col}/I_b);
- the thickness of the top (th_{tc}) and bottom (th_{bc}) flange cleat;
- the maximum thickness of right or left web cleat ($Max\text{-}th_{wc}$);
- the bolt size (d_b);
- the ratio of column to beam yield strength ($f_{y,c}/f_{y,b}$).

The statistical characteristics of these variables are summarized in Table 2.

Table 2. Characteristics of input and output parameters for artificial neural network (ANN) training.

Statistical Index		Type	Max	Min	Avg.	STD
I_{col}/I_b		Input	20.00	0.29	2.59	3.95
th_{tc}	(mm)	Input	15.90	0.00	8.10	4.79
th_{bc}	(mm)	Input	15.90	0.00	8.70	4.45
$Max\text{-}th_{wc}$	(mm)	Input	15.00	0.00	6.17	4.50
d_b	(mm)	Input	24.00	16.00	19.51	1.69
$f_{y,c}/f_{y,b}$		Input	1.13	0.79	0.99	0.08
$S_{j,ini}$	(kNm/rad)	Output	36,365.00	1633.00	12,021.75	9108.08
$M_n/M_{p,beam}$		Output	0.95	0.13	0.43	0.19

The number of hidden layers and the total number of neurons in the hidden layers in an ANN depend on the nature of the problem [51]. Generally, the trial and error method is used to obtain the ideal architecture that best reflects the characteristics of laboratory data. In this paper, an innovative method for calculating the number of neurons in hidden layers is taken into account, namely:

$$N_H \leq 2N + 1 \tag{9}$$

where N_H represents the number of neurons in the hidden layers and N_I is the number of input variables.

Since the number of influential input variables for the current study is equal to 6, the empirical Equation (9) shows that the number of neurons in hidden layers can be less than 13. Therefore, several networks with different topologies (with a maximum of two hidden layers and a maximum of 13 neurons) were trained and studied in this paper.

The hyperbolic tangent stimulation function and Levenberg–Marquardt training algorithm were used in all networks. The statistical indices used to evaluate the performance of different topologies are the root mean squared error (*RMSE*), the average absolute error (*AAE%*), the model efficiency (*EF*), and the variance account factor (*VAF%*) that are defined as follows [52]:

$$RMSE = \left[\frac{1}{n}\sum_{i=1}^{n}(P_i - O_i)^2\right]^{\frac{1}{2}} \tag{10}$$

$$AAE = \frac{\left|\sum_{i=1}^{n}\frac{(O_i - P_i)}{O_i}\right|}{n} \times 100 \tag{11}$$

$$EF = 1 - \frac{\sum_{i=1}^{n}(P_i - O_i)^2}{\sum_{i=1}^{n}\left(\overline{O}_i - O_i\right)^2} \tag{12}$$

$$VAF = \left[1 - \frac{var(O_i - P_i)}{var(O_i)}\right] \times 100 \tag{13}$$

After examining different topologies of networks, it was found that the network with a 6-7-6-1 topology is characterized by the lowest value of error in *RMSE*, *AAE%*, *EF*, and *VAF%*, and by the highest value of R^2 to estimate the two output parameters $S_{j,ini}$ and ($M_n/M_{p,beam}$), as also shown in Table 3. It is necessary to mention that the error criteria for training and testing the selected data are calculated in the main range of variables and not in the normal range.

In this study, as it is for several structural engineering practice applications, the ABC algorithm is used as a new metaheuristic algorithm to determine the weight optimization of each ANN model. In more detail, the ($M_n/M_{p,beam}$) output has a numerical range of 0–1 while the $S_{j,ini}$ output is characterized by a numerical range of 1600–37,000 (kNm/rad). This means that there is a big difference between the two target outputs. For modulation, two separate ANNs were hence used in this study, each one with one output. Their basic characteristics are summarized in Table 4.

Figure 7 shows the optimal topology of an FF network with two hidden layers, six input variables (neurons), and one output parameter. The ABC has been also used to provide the least prediction error for the trained structure, in order to optimize the weights and biases of the ANN model. The ABC parameters are also presented in Table 5.

Table 3. Statistical indices of ANN with best 6-7-6-1 topology, as combined with artificial bee colony (ABC).

Type	Statistical Index	$S_{j,ini}$ (kNm/rad)	$M_n/M_{p,beam}$
Train	R^2	0.922	0.955
	y = ax + b	y = 0.8107x + 2,037.8	y = 0.9319x + 0.033
	RMSE	3542.657	0.058
	AAE %	0.292	0.108
	EF	0.848	0.911
	VAF %	0.849	0.912
Test	R^2	0.939	0.954
	y = ax + b	y = 0.9406x + 2860.1	y = 0.8749x + 0.0303
	RMSE	3790.584	0.065
	AAE %	0.422	0.109
	EF	0.817	0.892
	VAF %	0.878	0.908
All	R^2	0.918	0.953
	y = ax + b	y = 0.8287x + 2257.6	y = 0.9142x + 0.0348
	RMSE	3592.297	0.059
	AAE %	0.317	0.108
	EF	0.842	0.908
	VAF %	0.843	0.908

Table 4. Structure and topology of the feed-forward (FF) neural network.

No.	Name	Features of Neural Network						
		Number of Input	Number of Output	Neural Network	Hidden Layer	Node	Learning Role	Transfer Function
1	ABC-ANN-s	6	1	FF	2	7-6	Levenberg–Marquardt	tansig
2	ABC-ANN-m	6	1	FF	2	7-6	Levenberg–Marquardt	tansig

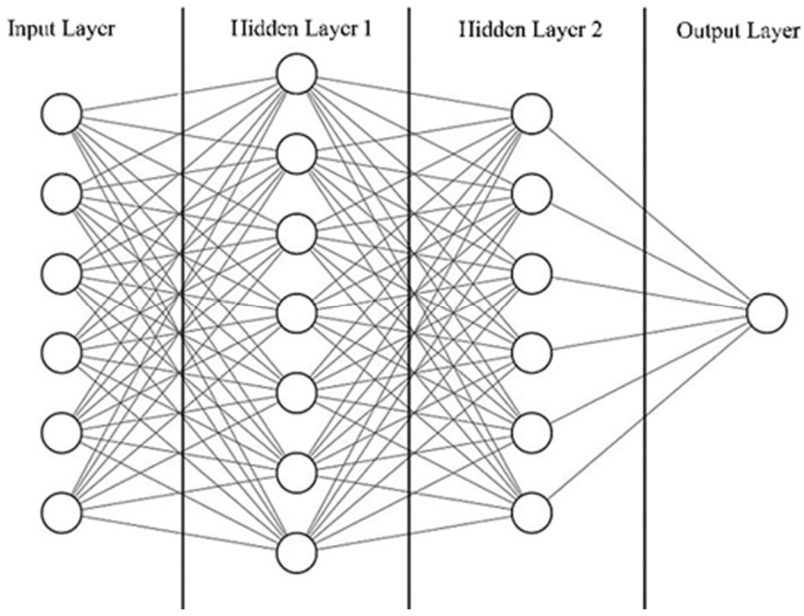

Figure 7. Feed-forward ANN with 6-7-6-1 structure.

Table 5. Features of ABC algorithm in the proposed ANN model.

No.	Name	Features of ABC Algorithm			
		Number of Bees	Source Number	Onlooker Number	Max Number of Cycles
1	ABC-ANN-S	50	25	25	100
2	ABC-ANN-M	30	15	15	150

6. Results and Discussion

6.1. Accuracy of Proposed ABC-ANN Model

Table 6 shows the comparison between different models with experimental data for estimating $S_{j,ini}$ and M_n. Concerning the calculated average ("Avg.") and standard deviation ("STD") values, the results in Table 6 indicate that the ABC-ANN model provides more reliable predictions for both, compared to the EC3 or KK formulations described earlier. Using the existing empirical models, in particular, the $S_{j,ini}$ and M_n predictions for some specimens are either underestimated or overestimated, and this suggests the limitation of mechanical models to capture the underlying mechanism that governs both the parameters. The ABC-ANN predictions, conversely, are characterized by minimum deviation.

Table 6. Comparison of different models with literature test data, as obtained in terms of $S_{j,ini}$ and M_n.

$S_{j,ini}$ (kNm/rad)				M_n (kNm)			
Test	Test/EC3	Test/KK	Test/ABC-ANN-S	Test	Test/EC3	Test/KK	Test/ABC-ANN-M
6000	0.62	0.81	1.32	43.6	1.11	1.22	0.91
13,846	0.44	1.49	0.57	44.9	0.93	0.95	0.92
10,099	0.49	1.03	0.78	54.2	1.11	1.22	0.73
1633	1.32	1.34	1.23	21.7	1.17	1.21	1.9
8089	1.65	1.26	0.98	43.3	1.02	1.09	0.95
4490	1.80	1.13	1.33	33.1	1.25	1.37	1.2
4638	1.17	0.96	1.7	47.4	1.34	1.47	0.87
6060	1.50	1.43	1.32	50.4	1.87	2.07	1.6
10,029	1.61	1.94	0.98	54.6	1.56	1.67	0.97
30,222	2.74	4.09	0.99	74.7	1.35	1.37	0.95
21,623	1.74	0.99	0.88	83.7	1.08	1.11	1.19
26,919	1.05	0.87	0.88	168.8	0.75	1.12	1.01
11,022	0.87	0.51	0.66	80.9	1.30	1.31	1.25
23,852	1.67	1.07	0.8	101.3	1.03	1.06	0.99
22,672	1.78	0.97	0.84	119.9	1.22	1.57	0.81
25,247	0.97	0.76	0.94	127.4	1.00	1.03	0.99
58,679	1.43	1.27	1.14	186.9	1.045	1.07	0.96
24,169	0.93	0.72	0.99	123.8	0.97	1.00	1.02
Avg.	1.32	1.26	1.01		1.17	1.27	1.02
STD	0.56	0.78	0.27		0.25	0.28	0.19

Figures 8 and 9 show the scatter graph that provided the relationship between test results and the proposed ABC-ANN model for estimating the $S_{j,ini}$ and M_n parameters, respectively. In this case, the comparative results also indicate that the ABC-ANN model offers a reliable value for the ratio of experimental to computational predictions (R^2), for both the examined mechanical parameters, and thus confirming further the high potential and accuracy of the proposed model.

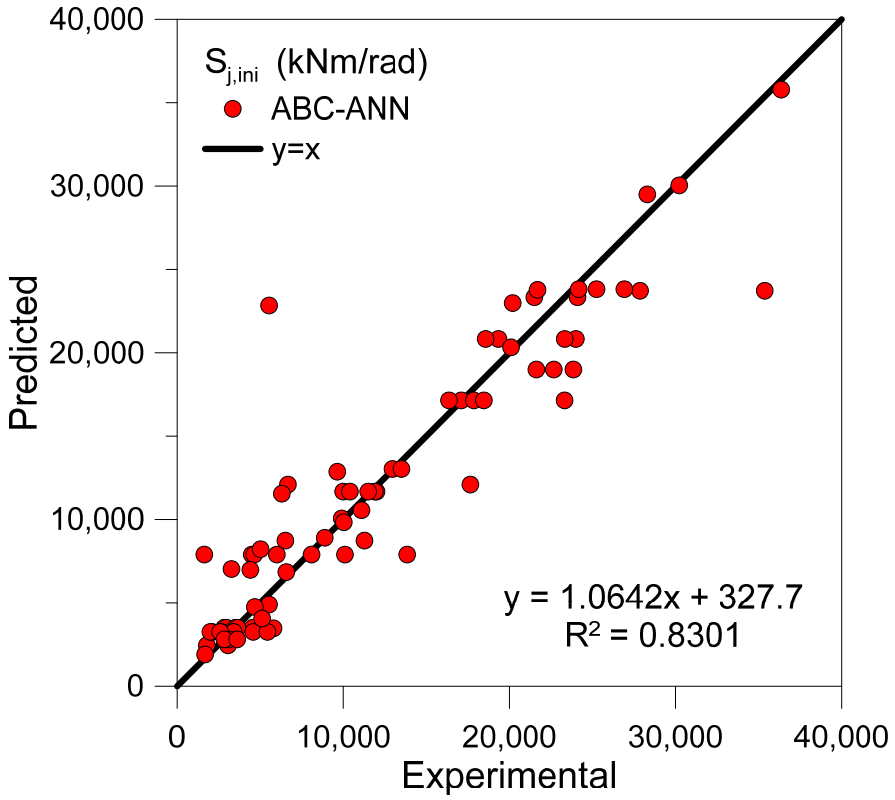

Figure 8. ABC-ANN calculated versus experimentally observed values for the parameter $S_{j,ini}$.

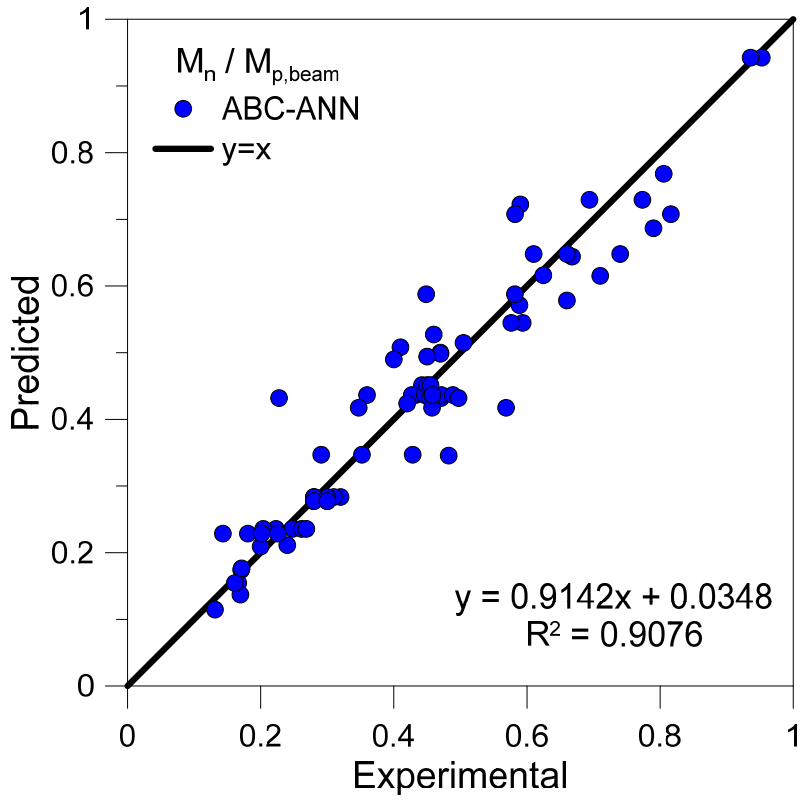

Figure 9. ABC-ANN calculated versus experimentally observed values for the parameter ($M_n/M_{p,beam}$).

In conclusion, Tables 7 and 8 provide the final weights and biases for both hidden layers, as estimated by the ABC-ANN model. Using the values of the weights and biases between the different ANN layers, the two output parameters ($S_{j,ini}$ and $M_n/M_{p,beam}$) can be determined and predicted.

Table 7. Final weights and bias values of the ABC-ANN model for $S_{j,ini}$ (kNm/rad).

IW						**b_1**
0.4817	0.1907	−0.2197	−0.4365	0.5490	−0.5109	0.9004
−0.3810	0.0292	0.5892	−0.2042	−0.7789	0.7893	0.5127
0.0253	0.0070	−0.7712	0.5666	−0.1401	0.8548	0.3646
0.8274	−0.7504	−0.8258	0.9904	−0.4542	−0.4942	−0.1958
0.5154	−1.0000	0.3092	0.4735	−0.5747	0.0010	0.0809
−0.8149	−0.0035	−0.6034	0.3425	1.0000	−0.0460	−0.4586
−0.4572	1.0000	0.3426	0.9226	−0.1067	−0.9320	1.0000
LW1						**b_2**
−0.8055	−0.7453	0.8586	−0.3097	0.5595	0.4411	−0.8149	−0.2254
0.9575	−1.0000	−0.7036	0.8996	−0.2134	−0.8109	−0.2879	0.8898
−0.6931	−0.0147	0.1303	−0.3631	0.3113	−0.3478	−0.5636	0.0838
-0.4409	−0.7401	0.4323	−0.9174	0.3017	−0.6847	−1.0000	0.5783
-0.4875	−0.0611	0.3553	−0.8939	1.0000	−0.5234	−0.5076	0.2355
0.5268	−1.0000	−0.7456	−0.1620	0.1855	−0.1735	−0.2715	0.2381
LW2						**b_3**
−0.8122	−0.2114	0.4500	0.1232	−0.9455	−0.1440		−0.8268

Table 8. Final weights and bias values of the ABC-ANN model for ($M_n/M_{p,beam}$).

IW						**b_1**
0.5052	0.026	−0.048	−0.457	−0.601	0.880	−0.263
0.0611	−0.002	0.231	1.000	−0.039	−0.041	−0.096
0.8044	0.613	0.636	−0.597	0.068	−0.707	0.830
−0.0309	0.840	1.000	0.972	0.503	0.902	0.328
−0.0211	−0.668	0.193	0.190	0.841	0.214	0.582
−0.8067	−0.706	0.351	−0.533	−0.137	0.048	0.332
0.6398	0.751	0.515	−0.311	0.908	−1.000	−0.874
LW1						**b_2**
−0.8170	0.552	−0.907	−0.003	0.750	−0.879	−0.423	−0.870
−0.8032	0.822	−1.000	−0.435	0.052	−0.235	0.438	−0.286
−0.7108	−0.702	−0.572	−0.039	0.144	0.154	0.653	0.159
−0.3023	−0.827	0.142	0.368	0.149	0.385	0.467	−0.822
0.6028	0.679	−0.656	−0.584	−0.243	−0.078	0.546	0.176
0.9051	−0.554	−0.576	−0.672	0.981	−0.221	−0.992	0.303
LW2						**b_3**
−0.4997	−0.239	0.875	−0.930	−0.243	−0.643		−0.930

IW: weight values for input layer; LW1: weight values for first hidden layer; LW2: weight values for second hidden layer; b_1: bias values for first hidden layer; b_2: bias values for second hidden layer; b_3: bias values for output layer.

To formulate ANN results, weights and biases from Tables 7 and 8 should be normalized as:

$$X_n = \frac{2 \times (X - X_{min})}{X_{max} - X_{min}} - 1 \quad (14)$$

By substituting the normalized values of Table 3 for each one of the six input parameters, they are represented by a 6×1 vector that is herein labeled as $a^{(1)}$. Then, by using the following equations, the values of $S_{j,ini}$ and $(M_n/M_{p,beam})$ can be calculated from:

$$a^{(2)} = tanh\left(IW \times a^{(1)} + b_1\right) \tag{15}$$

$$a^{(3)} = tanh\left(LW1 \times a^{(2)} + b_2\right) \tag{16}$$

$$Y_{S\ or\ M}^{Predic(Normalize)} = tanh\left(LW2 \times a^{(3)} + b_3\right) \tag{17}$$

$$Y_{S\ or\ M}^{Predict(Actual)} = \frac{Y_{S\ or\ M}^{Predict(Normalize)} + 1}{2} \times (Y_{max} - Y_{min}) + Y_{min} \tag{18}$$

The parameters IW, $LW1$, $LW2$, b_1, b_2, and b_3 are shown as vector matrices in Tables 7 and 8. Furthermore, "S" and "M" in Equations (15)–(18) stand for $S_{j,ini}$ and $(M_n/M_{p,beam})$, respectively.

Another visual measure that can be taken into account for comparing the performance of the ABC-ANN model against the component-based mechanical models (EC3 or KK) is the Taylor diagram, see Figures 10 and 11. This diagram depicts a graphical illustration of the adequacy of each investigated model, based on the root mean square-centered difference, the correlation coefficient, and the standard deviation.

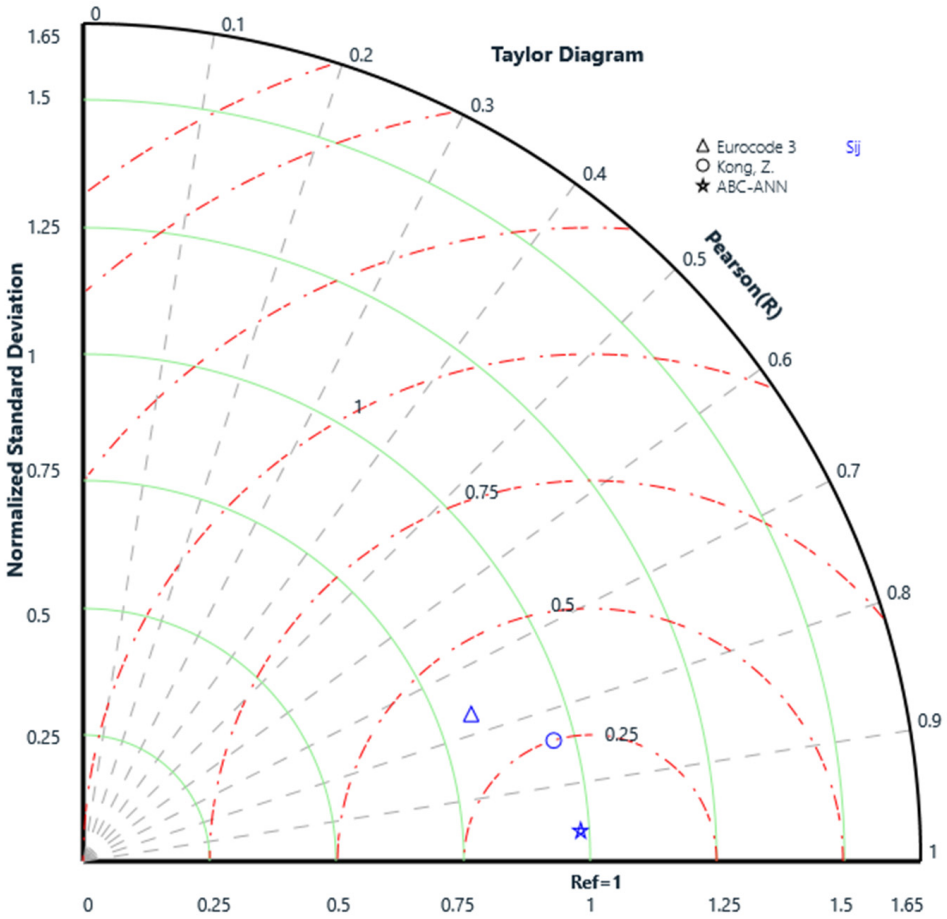

Figure 10. Taylor diagram visualization of model performance, in terms of $S_{j,ini}$ predictions.

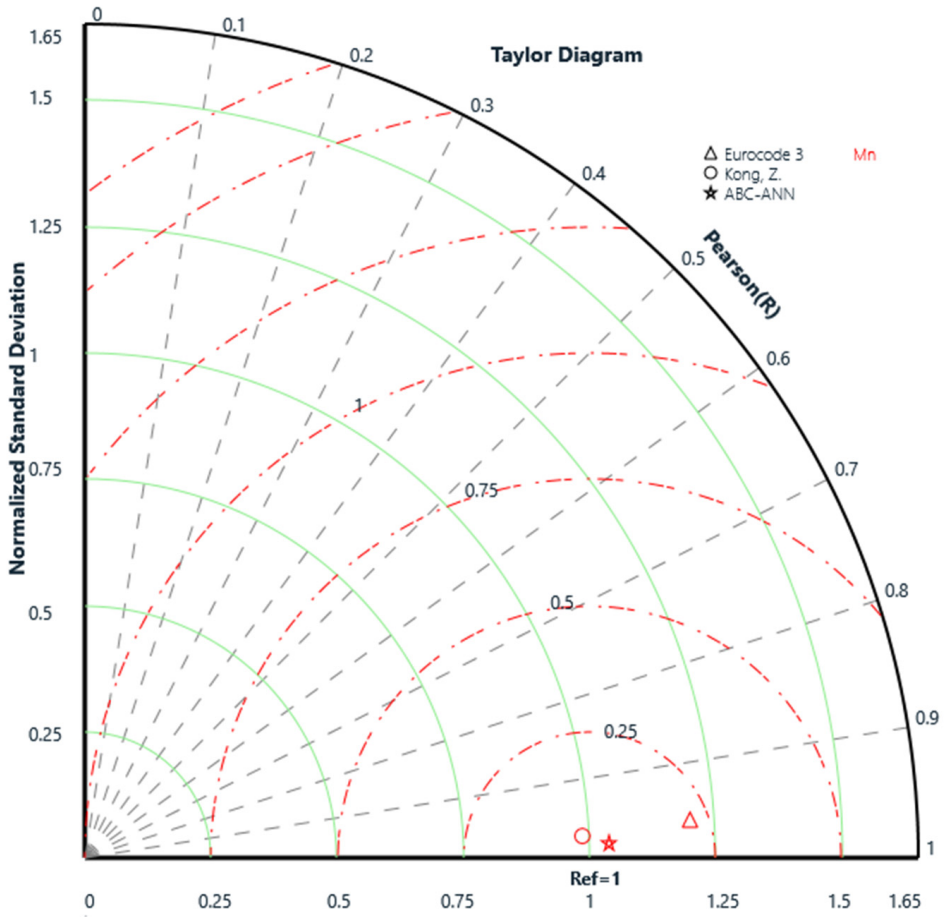

Figure 11. Taylor diagram visualization of model performance, in terms of M_n predictions.

The results shown in Figures 10 and 11 clearly indicate that the closest prediction for both the $S_{j,ini}$ and M_n input parameters, to the point representing the experimental data of the literature, are provided by the herein developed ABC-ANN model. The EC3 component-based model, as shown, also results in high values of root mean square-centered difference and standard deviation, thus further suggesting a good accuracy of the formulation over the selected experimental data. The same comparative parameters, conversely, are rather low regarding the application of the KK model to the selected experimental specimens.

6.2. Sensitivity Analysis

As previously discussed, the accuracy and potential of the proposed ABC-ANN model for the estimation of the $S_{j,ini}$ and M_n parameters in TSACWs was acknowledged by comparison with the EC3 and KK component-based formulations. In order to investigate in more detail the effect of all the required input parameters, a sensitivity analysis (SA) was carried out for the selected TSACW specimens. The SA reveals how significantly the model output can be affected by changes within input variables. There are two main types of SA, known as "global" and "local" sensitivity analyses, where the local sensitivity analysis (LSA) concentrates on the local impact of individual input parameters on the overall performance. The global sensitivity analysis (GSA), on the other hand, evaluates the influence of individual input parameters over their entire spatial range and measures the uncertainty of the overall performance (output) caused by input uncertainty, over interaction with other parameters, or also taken individually. Therefore, considering the nature of the complex non-linear behavior and variation of $S_{j,ini}$ and M_n parameters in the current study, the GSA was selected as much more rational for investigating the impact of input parameters on the overall performance.

Amongst GSA methods, a variance-based approach has been primarily considered in past literature for SA. The method provides a specific methodology for defining total and first-order sensitivity indices for each input parameter of the ANN model. Assuming a model in the form $Y = f(X_1, X_2, \ldots, X_k)$, where Y is scalar, the variance-based technique takes a variance ratio to evaluate the impact of individual parameters using variance decomposition as:

$$V = \sum_{i=1}^{k} V_i + \sum_{i=1}^{k} \sum_{j>i}^{k} V_{ij} + \ldots + V_{1,2,\ldots,k} \tag{19}$$

where V is the variance of the ANN model output; V_i is the first-order variance for the input X_i; V_{ij} to $V_{1,2,\ldots,k}$ correspond to the variance of the interaction of the k parameters.

V_i and V_{ij}, which denote the significance of the individual input to the variance of the output, are a function of the conditional anticipation variance:

$$V_i = V_{x_i}[E_{x_{\sim i}}(YX_i)] \tag{20}$$

$$V_{ij} = V_{x_i x_j}\left[E_{x_{\sim ij}}(YX_i, X_j)\right] - V_i - V_j \tag{21}$$

where the suffix $x_{\sim i}$ designates the set of all input variables apart from X_i.

The first-order sensitivity index (S_i) represents the first-order impact of an input X_i on the overall output provided by:

$$S_i = \frac{V_i}{V(Y)} \tag{22}$$

The abovementioned methodology for calculating the first-order sensitivity index was used in this research study. Major results of the SA are presented in Figure 12.

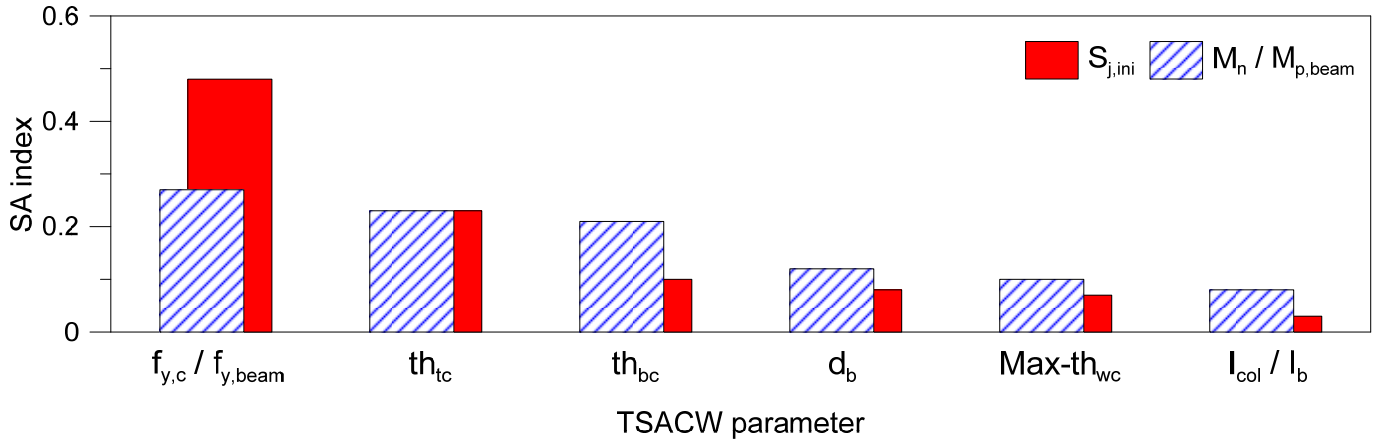

Figure 12. Sensitivity indices of variables $S_{j,ini}$ and ($M_n/M_{p,beam}$).

Apart from the yield strength (f_y) that depends on material properties, the comparative results indicate that the thickness of top flange (th_{tc}) has the most influence, while the moment inertia ratio of column to beam (I_{col}/I_b) has the least effect on both the output parameters, $S_{j,ini}$ and M_n. The thickness of the bottom flange cleat (th_{bc}) can be classified as the second most influential input variable, especially in terms of maximum moment capacity M_n.

7. Concluding Remarks

Modeling the plastic response of different components in beam-to-column bolted connections and their interactions is a challenging issue in the structural engineering community. In this paper, an informational artificial neural network (ANN) model combined with the metaheuristic artificial bee colony (ABC) algorithm was developed to model the initial stiffness ($S_{j,ini}$) and maximum moment capacity (M_n) of top-seat angle connections

with double web angles (TSACWs). Two different formulations of component-based mechanical models of the literature (as proposed by Eurocode 3 ("EC3") or by Kong and Kim in 2017 ("KK")) were also investigated in detail.

The discussed comparisons and results confirmed that the efficiency of the component-based mechanical model depends on the number and accuracy of the relationships of the constitutive components. By defining a sufficient number of components and subsequently idealizing the physical behavior in analytical equations, the reliable application of the mechanical model to different connection configurations is possible.

Nevertheless, idealization typically resulted in equations that excluded several important physical behavioral features of TSACWs, such as slippage. On the other hand, unlike the conventional mechanical modeling process that involves idealization from the observed behavior to the mathematical equations, in the informational base method, the information about essential behavior is extracted from available experimental test data and processed using an ANN. Nevertheless, the ANN model was limited to providing the global response only for bolted connections that include the contributions of all the constitutive components. Using this method, as shown, it is impossible to represent individual components and their actual contribution. Therefore, the model does not offer an insight into the underlying mechanics. Overall, the following conclusions can thus be derived:

- both the EC3 and KK component-based models failed to capture the underlying mechanism for estimating $S_{j,ini}$ and M_n parameters. As a result, these were either underestimated or overestimated for the reference specimens. On the other hand, the herein developed ABC-ANN model proved to offer a reliable prediction of required parameters, as also emphasized by the ratio of observational to computational values (R^2), and thus suggesting the high potential and accuracy of the proposal.
- The ANN model combined with the ABC algorithm established an excellent agreement with the available experimental database. The results highlighted that the ANN model may be a reliable alternative to a component-based mechanical model to estimate the mechanical behavior of bolted beam-to-column connections. Using the values of weights and biases between the different ANN layers, the two output parameters ($S_{j,ini}$ and M_n) can be accurately predicted.
- The sensitivity analysis confirmed that (apart from the yield strength f_y that necessarily depends on material properties) the thickness of the top flange (th_{tc}) has a significant influence, while the moment inertia ratio of column to beam (I_{col}/I_b) has the least effect on both the predicted output parameters, $S_{j,ini}$ and M_n.

Author Contributions: This research paper results from a joint collaboration of all the involved authors. All authors contributed to the paper drafting and review, I.F., M.N., R.P. and C.B. All authors have read and agreed to the published version of the manuscript.

Funding: This work was supported by funding from the Federal State Autonomous Educational Institution of Higher Education South Ural State University (National Research University). Further, MDPI is also acknowledged for providing waived fees (Guest Editor C.B.) in support of standard publication APCs.

Institutional Review Board Statement: The study did not require ethical approval.

Informed Consent Statement: Not applicable.

Data Availability Statement: Data sharing not applicable.

Conflicts of Interest: The authors declare no conflict of interest.

References

1. ANSI/AISC. *AISC 358-05 Prequalified Connections for Special and Intermediate Steel Moment Frames for Seismic Applications*; American Institute of Steel Construction Inc.: Chicago, IL, USA, 2005.
2. Madas, P.J.; Elnashai, A.S. A component-based model for beam-column connections. In Proceedings of the 10th World Conference of Earthquake Engineering, Madrid, Spain, 19–24 July 1992; pp. 4495–4499.
3. Chisala, M.L. Modelling M–φ curves for standard beam-to-column connections. *Eng. Struct.* **1999**, *21*, 1066–1075. [CrossRef]

4. Kim, J.; Ghaboussi, J.; Elnashai, A.S. Mechanical and informational modeling of steel beam-to-column connections. *Eng. Struct.* **2010**, *32*, 449–458. [CrossRef]
5. Pinheiro, L.; Silveira, R.A. Computational procedures for nonlinear analysis of frames with semi-rigid connections. *Lat. Am. J. Solids Struct.* **2005**, *2*, 339–367.
6. Hasan, M.J.; Ashraf, M.; Uy, B. Moment-rotation behaviour of top-seat angle bolted connections produced from austenitic stainless steel. *J. Constr. Steel Res.* **2017**, *136*, 149–161. [CrossRef]
7. Lacey, A.W.; Chen, W.; Hao, H.; Bi, K. Review of bolted inter-module connections in modular steel buildings. *J. Build. Eng.* **2019**, *23*, 207–219. [CrossRef]
8. Chen, Z.; Liu, J.; Yu, Y. Experimental study on interior connections in modular steel buildings. *Eng. Struct.* **2017**, *147*, 625–638. [CrossRef]
9. Chua, Y.; Liew, J.R.; Pang, S. Modelling of connections and lateral behavior of high-rise modular steel buildings. *J. Constr. Steel Res.* **2020**, *166*, 105901. [CrossRef]
10. Lacey, A.W.; Chen, W.; Hao, H.; Bi, K. New interlocking inter-module connection for modular steel buildings: Simplified structural behaviours. *Eng. Struct.* **2021**, *227*, 111409. [CrossRef]
11. Thai, H.-T.; Vo, T.P.; Nguyen, T.-K.; Pham, C.H. Explicit simulation of bolted endplate composite beam-to-CFST column connections. *Thin-Walled Struct.* **2017**, *119*, 749–759. [CrossRef]
12. Natesan, V.; Madhavan, M. Experimental study on beam-to-column clip angle bolted connection. *Thin-Walled Struct.* **2019**, *141*, 540–553. [CrossRef]
13. En, B. *1-8: 2005. Eurocode 3: Design of Steel Structures-Part 1-8: Design of Joints*; British Standards Institution: London, UK, 2005.
14. Kong, Z.; Kim, S.-E. Moment-rotation behavior of top-and seat-angle connections with double web angles. *J. Constr. Steel Res.* **2017**, *128*, 428–439. [CrossRef]
15. Calado, L.; De Matteis, G.; Landolfo, R. Experimental response of top and seat angle semi-rigid steel frame connections. *Mater. Struct.* **2000**, *33*, 499–510. [CrossRef]
16. Wang, T.; Song, G.; Liu, S.; Li, Y.; Xiao, H. Review of Bolted Connection Monitoring. *Int. J. Distrib. Sens. Netw.* **2013**, *9*, 871213. [CrossRef]
17. Jiang, L.; Rasmussen, K.; Zhang, H. Experimental investigation of full-range action-deformation behaviour of top-and-seat angle and web angle connections. In Proceedings of the 9th international conference on Advances in Steel Structures, Hong Kong, China, 5–7 December 2018.
18. Yan, S.; Jiang, L.; Rasmussen, K.J. Full-range behaviour of double web angle connections. *J. Constr. Steel Res.* **2020**, *166*, 105907. [CrossRef]
19. Kong, Z.; Kim, S.-E. Numerical Estimation for Initial Stiffness and Ultimate Moment of Top-Seat Angle Connections without Web Angle. *J. Struct. Eng.* **2017**, *143*, 04017138. [CrossRef]
20. Hasan, M.J.; Al-Deen, S.; Ashraf, M. Behaviour of top-seat double web angle connection produced from austenitic stainless steel. *J. Constr. Steel Res.* **2019**, *155*, 460–479. [CrossRef]
21. Kim, J.H. *Hybrid Mathematical and Informational Modeling of Beam-to-Column Connections*; University of Illinois at Urbana-Champaign: Champaign, IL, USA, 2010.
22. Moradi, S.; Alam, M.S. Finite-Element Simulation of Posttensioned Steel Connections with Bolted Angles under Cyclic Loading. *J. Struct. Eng.* **2016**, *142*, 04015075. [CrossRef]
23. Amadio, C.; Bedon, C.; Fasan, M.; Pecce, M.R. Refined numerical modelling for the structural assessment of steel-concrete composite beam-to-column joints under seismic loads. *Eng. Struct.* **2017**, *138*, 394–409. [CrossRef]
24. Málaga-Chuquitaype, C.; Elghazouli, A. Component-based mechanical models for blind-bolted angle connections. *Eng. Struct.* **2010**, *32*, 3048–3067. [CrossRef]
25. Azizinamini, A.; Radziminski, J.B. Static and Cyclic Performance of Semirigid Steel Beam-to-Column Connections. *J. Struct. Eng.* **1989**, *115*, 2979–2999. [CrossRef]
26. Pucinotti, R. Cyclic mechanical model of semirigid top and seat and double web angle connections. *Steel Compos. Struct.* **2006**, *6*, 139–157. [CrossRef]
27. Azizinamini, A.; Bradburn, J.; Radziminski, J. Initial stiffness of semi-rigid steel beam-to-column connections. *J. Constr. Steel Res.* **1987**, *8*, 71–90. [CrossRef]
28. Kishi, N. *Moment-Rotation Relation of Top-and Seat-Angle with Double Web-Angle Connections*; School of Civil Engineering, Purdue University: West Lafayette, IN, USA, 1987.
29. Kishi, N.; Chen, W. Moment-Rotation Relations of Semirigid Connections with Angles. *J. Struct. Eng.* **1990**, *116*, 1813–1834. [CrossRef]
30. Pucinotti, R. Top-and-seat and web angle connections: Prediction via mechanical model. *J. Constr. Steel Res.* **2001**, *57*, 663–696. [CrossRef]
31. Shen, J.; Astaneh-Asl, A. Hysteresis model of bolted-angle connections. *J. Constr. Steel Res.* **2000**, *54*, 317–343. [CrossRef]
32. De Stefano, M.; De Luca, A.; Astaneh-Asl, A. Modeling of Cyclic Moment-Rotation Response of Double-Angle Connections. *J. Struct. Eng.* **1994**, *120*, 212–229. [CrossRef]
33. Danesh, F.; Pirmoz, A.; Daryan, A.S. Effect of shear force on the initial stiffness of top and seat angle connections with double web angles. *J. Constr. Steel Res.* **2007**, *63*, 1208–1218. [CrossRef]

34. Pirmoz, A. Moment–rotation behavior of bolted top–seat angle connections. *J. Constr. Steel Res.* **2009**, *65*, 973–984. [CrossRef]
35. SALEM, A.H. *Behavior and Design of Steel I-beam-to-Column Flushed Rigid Bolted Connections*; The American University: Cairo, Egypt, 2011.
36. Weynand, K.; Huter, M.; Kirby, P.A.; Simoes da Silva, L.A.P. SERICON–Databank on Joints in Building Frames. In Proceedings of the 1st COST C1 Workshop—International Conference on Control of the Semi-Rigid Behaviour of Civil Engineering Structural Connections, Liège, Belgium, 17–19 September 1998; pp. 217–228.
37. Kishi, N.; Chen, W.-F. *Data Base of Steel Beam-to-Column Connections*; Structural Engineering Area, School of Civil Engineering, Purdue University: West Lafayette, IN, USA, 1986.
38. Astaneh, A. Demand and supply of ductility in steel shear connections. *J. Constr. Steel Res.* **1989**, *14*, 1–19. [CrossRef]
39. Construction, A.I.O.S. *Seismic Provisions for Structural Steel Buildings*; American Institute of Steel Construction: Chicago, IL, USA, 2002.
40. Komuro, M.; Kishi, N.; Chen, W. *Elasto-Plastic FE Analysis on Moment-Rotation Relations of Top-and Seat-Angle Connections*; Connections in Steel Structures V: Amsterdam, The Netherlands, 2004; pp. 111–120.
41. Faella, C.; Piluso, V.; Rizzano, G. *Prediction of the Flexural Resistance of Bolted Connections with Angles*; IABSE Reports; 1996; pp. 309–318. Available online: https://structurae.net/en/literature/conference-paper/prediction-of-the-flexural-resistance-of-bolted-connections-with-angles (accessed on 1 February 2021).
42. Flood, I.; Kartam, N. Neural Networks in Civil Engineering. I: Principles and Understanding. *J. Comput. Civ. Eng.* **1994**, *8*, 131–148. [CrossRef]
43. Kulkarni, P.; Londhe, S.; Deo, M. Artificial Neural Networks for Construction Management: A Review. *Soft Comput. Civ. Eng.* **2017**, *1*, 70–88.
44. Asteris, P.G.; Nikoo, M. Artificial bee colony-based neural network for the prediction of the fundamental period of infilled frame structures. *Neural Comput. Appl.* **2019**, *31*, 4837–4847. [CrossRef]
45. Hasanzade-Inallu, A.; Zarfam, P.; Nikoo, M. Modified imperialist competitive algorithm-based neural network to determine shear strength of concrete beams reinforced with FRP. *J. Central South Univ.* **2019**, *26*, 3156–3174. [CrossRef]
46. Haykin, S. *Neural Networks: A Comprehensive Foundation*; Prentice Hall: Upper Saddle River, NJ, USA, 1999.
47. Bishop, C.M. *Pattern Recognition and Machine Learning*; Springer: New York, NY, USA, 2006.
48. Najimi, M.; Ghafoori, N.; Nikoo, M. Modeling chloride penetration in self-consolidating concrete using artificial neural network combined with artificial bee colony algorithm. *J. Build. Eng.* **2019**, *22*, 216–226. [CrossRef]
49. Karaboga, D.; Basturk, B. On the performance of artificial bee colony (ABC) algorithm. *Appl. Soft Comput.* **2008**, *8*, 687–697. [CrossRef]
50. Karaboga, D.; Akay, B. A comparative study of Artificial Bee Colony algorithm. *Appl. Math. Comput.* **2009**, *214*, 108–132. [CrossRef]
51. Asteris, P.; Plevris, V. Neural Network Approximation of the Masonry Failure under Biaxial Compressive Stress. In Proceedings of the SEECCM III-3rd South-East European Conference on Computational Mechanics-an ECCOMAS and IACM Special Interest Conference, Kos Island, Greece, 12–14 June 2013.
52. Li, J.; Heap, A.D. *A Review of Spatial Interpolation Methods for Environmental Scientists*; Record 2008/23; Geoscience Australia: Canberra, Australia, 2008; p. 137.